

## Clumpy Flows in Protoplanetary and Planetary Nebulae

Alexei Y. Poludnenko<sup>1</sup> and Adam Frank<sup>2</sup>

*Department of Physics and Astronomy, University of Rochester,  
Rochester, NY 14627-0171*

Sorin Mitran<sup>3</sup>

*Department of Mathematics, University of North Carolina, CB #3250,  
Chapel Hill, NC 27599*

**Abstract.** Many astrophysical flows occur in inhomogeneous media. We briefly discuss some general properties of the adiabatic and radiative inhomogeneous systems and discuss the relevance of those properties to the planetary nebulae systems. We then focus on radiative hypersonic bullets and the applicability of this model to planetary and protoplanetary systems such as CRL 618, NGC 6543, Hen 3-1475.

### 1. Introduction

Recently it has been more and more widely acknowledged that it is important to consider the inhomogeneous structure of stellar outflows since "clumps", or "clouds", arising on a variety of scales can introduce not only quantitative but also qualitative changes to the overall dynamics of the flow. Planetary nebulae are an important astrophysical example of flows where the presence of inhomogeneities may play a conspicuous role in defining nebular dynamics and morphology.

Embedded inhomogeneities may come in two flavors. One includes large stationary or quasi-stationary ensembles of condensations, oftentimes forming extended shells. These may interact with the ambient flow, e.g. cometary knot shells in NGC 7293 (Helix) or NGC 2392 (Eskimo). The other includes more localized systems that consist of one or several compact knots or ejecta moving at significant velocities relative to the ambient medium. One of the most spectacular examples of such nebular systems is CRL 618, which exhibits long thin shocked lobes. The most prominent features of the lobes are their high length-to-width ratio and the presence of the periodic rings in their structure. There is also some evidence for a velocity increase in the lobes from the base to the tip (Sánchez Contreras, Sahai, & Gil de Paz 2002). Other examples include

---

<sup>1</sup>wma@pas.rochester.edu

<sup>2</sup>afrank@pas.rochester.edu

<sup>3</sup>mitran@amath.unc.edu

strings in NGC 6543 (Weis, Duschl, & Chu 1999) and knots in the outflow of Hen 3-1475 (Riera *et al.*2003).

## 2. Adiabatic vs. Radiative Systems

When the interaction of an inhomogeneity with a global flow proceeds in the adiabatic regime the dominant process is the *lateral clump re-expansion* (Klein, McKee, & Colella 1994; Poludnenko, Frank, & Blackman 2002). The internal shock compresses the clump which then re-expands in the lateral direction. Such re-expansion, in combination with instabilities at the upstream clump surface, is responsible for the destruction of the clump.

When more than one clump is present, lateral re-expansion also drives interclump interactions via merging and formation of larger structures that subsequently alter the global flow (Poludnenko *et al.*2002). We refer the reader to Poludnenko *et al.*(2002) for further details on the dynamics of the adiabatic inhomogeneous systems. We note that two key regimes can be defined: “*interacting*” and “*noninteracting*” systems. Clumps in the interacting systems will merge via lateral re-expansion before the clumps are destroyed.

Radiatively cooled inhomogeneous systems show a minimal role of lateral re-expansion and, therefore, of interclump interaction. The dominant process is the formation of instabilities with small wavelength at the bullet upstream surface. Hydrodynamic instabilities (Richtmeyer-Meshkov, Rayleigh-Taylor) produce the initial instability seed. The resulting density variations quickly trigger the onset of thermal instabilities which thereafter drive clump fragmentation.

The fragments produced by the instability are of different mass with the most massive ones being closest to the symmetry axis and the outermost ones being the lightest. As a result fragments are “peeled off” from the clump starting with those outermost in radius. When considering a single axisymmetric clump or bullet, each fragmentation event results in the formation of a distinct “*ring-like*” feature in the clump wake. The formation of rings is a consequence of the axisymmetry. In 3-D it is likely that the rings would themselves fragment (Klein *et al.*2003).

## 3. Radiative Bullet Simulations

Here we present a simulation of the propagation of a hypersonic radiative bullet as an example of a simple strongly cooled inhomogeneous system. Since, as it was mentioned above, the evolution of radiative inhomogeneous systems proceeds mostly in the noninteracting regime, the case of a single bullet can be considered a “building block” of more complicated inhomogeneity configurations. The simulation was performed with the AstroBEAR code based on the BEARCLAW adaptive mesh refinement package. Radiative cooling was tracked via a standard cooling curve. We refer the reader to (Poludnenko, Frank, & Mitran 2003) for further details on the model and the simulation.

The initial bullet radius is  $r_b = 3.0 \cdot 10^{15}$  cm, the initial bullet density is  $\rho_b = 10^5 \text{ cm}^{-3}$ . This translates into the initial bullet mass  $m_b \approx 0.5 \cdot 10^{-5} M_\odot$ . The initial bullet Mach number is  $M_b = 20$ , or  $v_b \approx 235 \text{ km s}^{-1}$ . The computational domain is of size  $1.8 \cdot 10^{17} \text{ cm} \times 2.4 \cdot 10^{16} \text{ cm}$  or expressed in terms of bullet

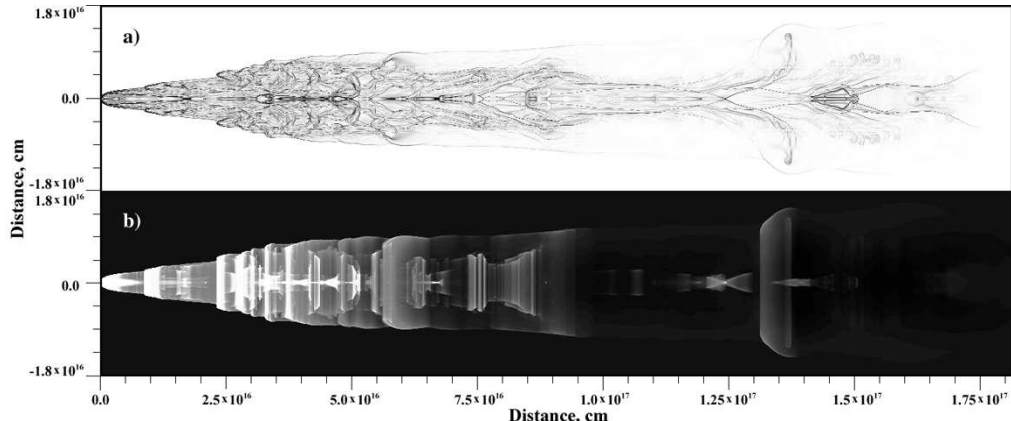


Figure 1. a) Synthetic Schlieren image of the computational domain at time 251.1 yrs. Shown is the gradient of the density logarithm. b) Synthetic observation image of the computational domain for the same time as in a). Note the periodic ring-like structures in the domain resulting from individual fragmentation episodes.

radii  $60r_b \times 8r_b$ . The ambient density is  $\rho_a = 1000 \text{ cm}^{-3}$  and the ambient temperature  $T_a = 10^4 \text{ K}$ . The run was carried out in cylindrical symmetry with the x-axis being the symmetry axis. We use an adaptive grid with 4 levels of refinement with equivalent resolution of  $1024 \times 7680$  cells.

In the simulation the hydrodynamic timescale, i.e. the bullet crushing time, was  $t_{hydro} = 2.54 \cdot 10^9 \text{ s} \approx 80.5 \text{ yrs.}$ , the cooling timescale was  $t_{cool} = 70.9 \cdot 10^3 \text{ s} \approx 19.7 \text{ hours}$ . The simulation total run time was  $9.49 \cdot 10^9 \text{ s} \approx 251.1 \text{ yrs.}$  Thus the evolution of the system was in a regime strongly dominated by cooling.

Figure 1 shows the computational domain at time  $t = 251.1 \text{ yrs.}$  In Figure 1a the synthetic Schlieren image (gradient of the density logarithm) is shown illustrating the shock and vortex sheet structure in the flow. Figure 1b shows the synthetic observation image of the computational domain. It represents the 2D projected distribution of the logarithm of the emissivity  $I = n^2 \Lambda$  integrated in the z-direction, where  $n$  is the number density and  $\Lambda$  is the cooling function. Note the presence of several characteristic ring-like structures in Figure 1b in the bullet wake, resulting from the fragmentation events.

Another key property of such systems is the presence of Hubble-type flows in the bullet wake. The left panel of Figure 2 shows the distribution of the total velocity  $v_{tot}(x)$  along the symmetry axis as a function of distance from the bullet head. The linear velocity decrease from the maximum value of  $210 \text{ km s}^{-1}$  from head to base is clear aside from some minor fluctuations arising due to the unsteadiness of the downstream flow. However, a better-founded comparison with observational data needs quantities more closely resembling observations. As an example, we consider the emissivity-weighted total velocity  $v_{emis}(x)$ , which is shown in the right panel of Figure 2. While it is significantly more noisy than the total velocity, the local maxima roughly fall on the same line as in the left panel giving some indication of a Hubble-type flow. It should be emphasized that we found evidence of Hubble flows only in systems dominated by radiative

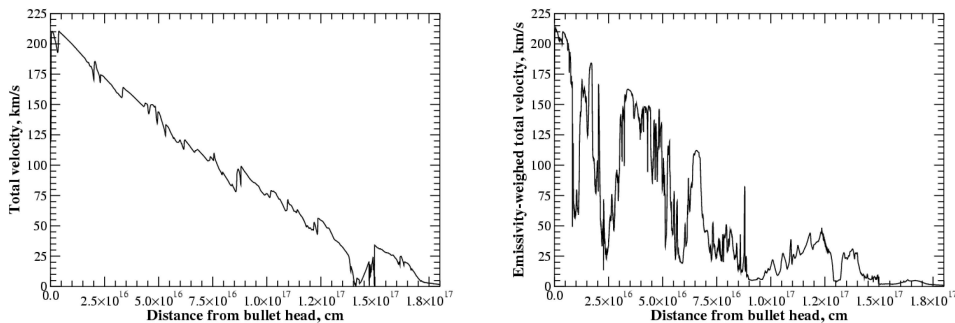


Figure 2. *Left*: distribution of total velocity along the symmetry axis of the bullet at the time 251.1 yrs. (same time in the simulation as the one shown in Figure 1). *Right*: distribution of the emissivity-weighted total velocity in the system at the same time.

cooling, i.e. where the ratio of the cooling time scale over the hydrodynamic time scale is  $\lesssim 1$ .

For radiative systems our principal conclusions are: (1) due to the lack of lateral re-expansion such systems evolve mostly in the noninteracting regime; (2) hypersonic radiative bullets are capable of producing structures with high length-to-width ratios (between 6 and 10 for our study); (2) the dominant process responsible for bullet destruction is instability formation at the bullet upstream interface leading to separate fragmentation episodes which create periodic “ring-like” structures in the wake; (3) simulations of strongly cooled systems show the presence of Hubble-type flows. How these flows appear observationally remains an open question. These properties suggest that hypersonic radiative bullets can be a likely candidate for a model of such systems as shocked lobes of CRL 618, strings of NGC 6543, etc.

This research was supported in part by the NSF grant AST-9702484, NASA grant NAG5-8428, HST Grants, DOE and the Laboratory for Laser Energetics under DOE sponsorship.

Animations can be found at <http://www.pas.rochester.edu/~wma>.

## References

- Klein, R. I., McKee, C. F., Colella, P. 1994, ApJ, 420, 213  
 Klein, R. I., Budil, K. S., Perry, T. S., Bach, D. R. 2003, ApJS, 583, 245  
 Poludnenko, A. Y., Frank, A., Blackman, E. G. 2002, ApJ, 576, 832  
 Poludnenko, A. Y., Frank, A., Mitran, S. 2003, ApJ, submitted (astro-ph/0310007)  
 Riera, A., García-Lario, P., Manchado, A., Bobrowsky, M., Estalella, R. 2003, A&A, 401, 1039  
 Sánchez Contreras, C., Sahai, R., Gil de Paz, A. 2002, ApJ, 578, 269  
 Weis, K., Duschl, W. J., Chu, Y.-H. 1999, A&A, 349, 467